DEVELOPMENT OF A 3D ELECTROMAGNETIC MODEL FOR EDDY CURRENT TUBING INSPECTION: APPLICATION TO STEAM GENERATOR TUBING

G. Pichenot[1], D. Prémel[1], T. Sollier[1], V. Maillot[2]

[1]C.E.A. Saclay, 91191 Gif-sur-Yvette, France
[2]I.R.S.N, 92262 Fontenay-aux-Roses, France

ABSTRACT. In nuclear plants, the inspection of heat exchanger tubes is usually carried out by using eddy current nondestructive testing. A numerical model, based on a volume integral approach using the Green's dyadic formalism, has been developed, with support from the French Institute for Radiological Protection and Nuclear Safety, to predict the response of an eddy current bobbin coil to 3D flaws located in the tube's wall. With an aim of integrating this model into the NDE multi techniques platform CIVA, it has been validated with experimental data for 2D and 3D flaws.

INTRODUCTION

The inspection of heat exchanger tubes is usually carried out by using eddy current (EC) nondestructive testing. This technique, based on the analysis of changes in the impedance of one or more coils placed inside the tube, is used to detect and characterize possible flaws or anomalies in the tube. In this context, for bobbin coils moving on the axis of the tube, many works have been done on the development of axisymmetric models in order to predict EC signals for circumferential flaws [1, 2, 3]. Others works, based on the Green's dyadic formalism [4, 5], are focused on 3D volumetric flaws by using volume integral models. In most investigated models, the axis of the driving coil is assumed to be coaxial with the axis of the inspected tube. Some recent works consider the EC problem of a conducting tube inspected by an eccentric circular coil [6, 7, 8, 9]. However, these works highlight the computation of the induced field in the tube's wall or the impedance of the coil without considering any flaw.

This paper describes the progress in developing a 3D computer code based on the volume integral method which has the capability to predict quickly the response of an eddy current probe to 3D flaws. This model is suitable to predict the probe response when the probe moves straight along the tube axis. The model can also be used to quantitatively evaluate perturbation factors on the eddy current signal such as the probe wobble (off-axis response for a non-centered bobbin coil configuration). The model gives the eddy currents distribution within the tube's wall and the changes in self and mutual inductance due to 3D flaws. 3D flaws are described as a local variation of conductivity which may vary by the shape, the size and the place in the tube's wall.
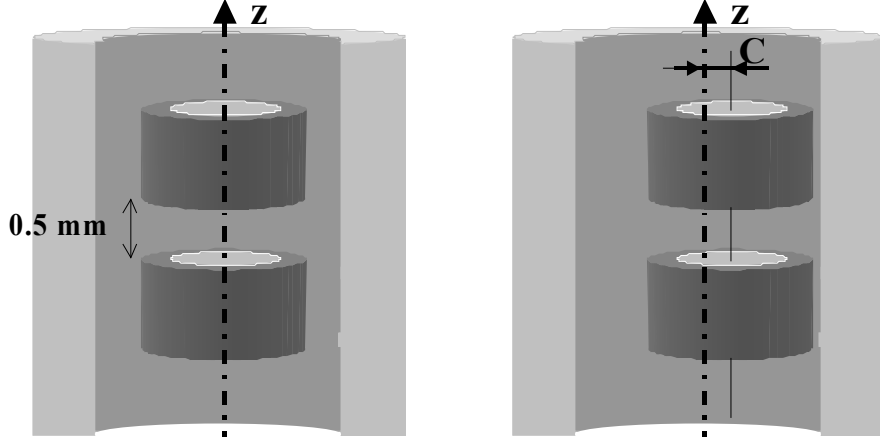
FIGURE 1. Schematic of the two bobbin coils probe used to inspect a conducting tube. The tube, made of inconel 600 (conductivity of 1 MS/m), has an inner radius of 9.84 mm and a thickness of 1.27 mm. The probe consists of two identical coils excited with a time harmonic drive current in phase in both coils (additive flux mode). The inner radius of the coils is 7.83 mm, the outer radius is 8.5 mm, the height is 2 mm, the number of turns is 70, the gap between the coils is 0.5 mm. The probe may moves straight along the tube axis (at left) or it may be non centered on the tube axis considering an eccentricity C (at right).

The probe can as well operate in absolute mode as in differential mode or pseudo absolute mode with additive or subtractive flux. To illustrate the matter, the configuration considered in this paper is given in Figure 1.

With an aim of integrating this model into the NDE multi techniques platform CIVA for an industrial use, the model has been validated with experimental data for 2D and 3D flaws.

THE VOLUME INTEGRAL FORMULATION

The inspected workpiece is a linear, isotropic, non-magnetic and conducting circular tube (permittivity ϵ_0, permeability μ_0, conductivivity σ_0) placed along the z-axis of a cylindrical coordinate system (r, θ, z). The probe is located inside the tube (region D_1) and excited by a time harmonic current of amplitude I and angular frequency ω. A 3D flaw is considered within the tube's wall (Region D_2) by local changes in the conductivity $\sigma(\mathbf{r})$. The electric field $\mathbf{E}_2(\mathbf{r})$ in region D_2 can be separated in two vectors $\mathbf{E}_2(\mathbf{r}) = \mathbf{E}_2^i(\mathbf{r}) + \mathbf{E}_2^p(\mathbf{r})$ and the forward problem is therefore treated in two steps. The first vector represents the incident field due to the current sources when there is no flaw while the second one is the perturbed field $\mathbf{E}_2^p(\mathbf{r})$ due to the presence of the flaw. So, the first step consists in computing the incident field $\mathbf{E}_2^i(\mathbf{r})$ in region D_2 due to the currents sources when there is no flaw, taking into account or not the eccentricity of the probe. The flaw problem can be handled in a similar way by considering the flaw is equivalent to a fictitious source of current $\mathbf{J}_2(\mathbf{r}) = [\sigma_0 - \sigma(\mathbf{r})]\mathbf{E}_2(\mathbf{r})$ which can be seen as a current dipole density. The perturbation field $\mathbf{E}_2^p(\mathbf{r})$ within the flaw domain Ω satisfies the Helmholtz equation:

$$\nabla \times \nabla \times \mathbf{E}_2^p - i\omega\mu_0\sigma_0\mathbf{E}_2^p = i\omega\mu_0\mathbf{J}_2(\mathbf{r}) \tag{1}$$

The integral solution of this equation involves the electric-electric dyadic's kernel $\overline{\mathbf{G}}_{ij}^{(ee)}(\mathbf{r}, \mathbf{r'})$ where the subscripts i and j denote respectively the region of observation and source. For canonical geometries, such as cylindrically layered media, the dyadic Green's functions can be found in explicit analytical expression [10]. The total internal electric field in region D_2 is obtained by the superposition of the incident field $\mathbf{E}_2^i(\mathbf{r})$ and the perturbed field $\mathbf{E}_2^p(\mathbf{r})$:

$$\mathbf{E}_2(\mathbf{r}) = \mathbf{E}_2^i(\mathbf{r}) + j\omega\mu_0 \int_{\text{flaw}} \overline{\mathbf{G}}_{22}^{(ee)}(\mathbf{r},\mathbf{r'})\left[\sigma(\mathbf{r'}) - \sigma_0\right]\mathbf{E}_2(\mathbf{r'})d\mathbf{r'} \tag{2}$$

A discrete solution of this integral equation is obtained by application of a Galerkin variant of the method of moments involving a suitable discretization of the flaw domain. The incident electric field may be also expressed by an integral equation [10]:

$$\mathbf{E}_2^i(\mathbf{r}) = j\omega\mu_0 \int_{\text{coil}} \overline{\mathbf{G}}_{21}^{(ee)}(\mathbf{r},\mathbf{r'}) \cdot \mathbf{J}_s(\mathbf{r'})d\mathbf{r'} \tag{3}$$

where $\overline{\mathbf{G}}_{21}^{(ee)}(\mathbf{r},\mathbf{r'})$ is the dyadic Green's functions corresponding to a source in region D_1 and the field observed in the region D_2. When the probe moves straight along the tube axis, the incident field calculation is straight forward by using Dodd and Deeds results valid for configuration with axial symmetry [1]. On the other hand, when the probe is non centered on the tube axis, the expressions of the current density in Equation (3) has to be written in the cylindrical system (r, θ, z) related to the tube axis [8].

By using the reciprocity principle which involves the incident electric field and the internal electric field in region D_2, the changes in self and mutual inductances ΔZ_{jk} due to 3D flaws is given for each coil by:

$$\Delta Z_{jk} = \frac{1}{I^2} \int_{\text{flaw}} \left[\sigma(\mathbf{r}) - \sigma_0\right] \mathbf{E}_{2(k)} \cdot \mathbf{E}_{2(j)}^i \; d\mathbf{r} \tag{4}$$

where $\mathbf{E}_{2(j)}^i$ is the incident field only produced by the coil (j) and $\mathbf{E}_{2(k)}$ is the internal field produced when the tube is only excited by the coil (k).

EXPERIMENTAL SETUP

As the changes in self and mutual inductances are very small, the measurements are usually done by using a Wheatstone bridge. The probe operates in differential mode at 100 kHz, 240 kHz and 500 kHz and in pseudo absolute mode at 100 kHz.

DIFFERENTIAL OPERATING MODE

In differential operating mode, the system is excited by a voltage V while the quantity which is measured is the voltage U.

As it has already been mentioned by Dodd and Deeds [1], in this mode the experimental setup has no significant influence on the measurements and the measurement is proportional to difference of the changes of impedance due to the flaw:

$$U = (\Delta Z_{11} - \Delta Z_{22}) \times \frac{i}{2} \tag{5}$$

PSEUDO ABSOLUTE OPERATING MODE

In pseudo absolute operating mode, the system is excited by a voltage V while the quantity which is measured is the terminal voltage (denoted U_1) of one of the two coils.

By considering only the two coils, the expression of U_1 is given by:

$$U_1 = (Z_{11} + Z_{12}) \times \frac{i}{2}$$

<div align="right">(6)</div>

RESULTS

In order to validate this numerical model, the simulated results were compared with experimental data. The EC signals are normalized with a 1 mm width 40% through wall outer groove (OG40). The simulated results have been validated with experimental data with various circumferential defects (Figure 2) as the 1 mm width 10% through wall inner groove (IG10).

As these flaws are circumferential defects, these configurations are 2D problems when the probe is centered in the tube. The results obtained with the 3D model in these configurations can thus also be compared with data obtained with a previous 2D computer modeling tool CIVA [3].

The results obtained with the 3D model have been validated with experimental data with various 3D defects by always normalizing the EC signal with the OG40 flaw.
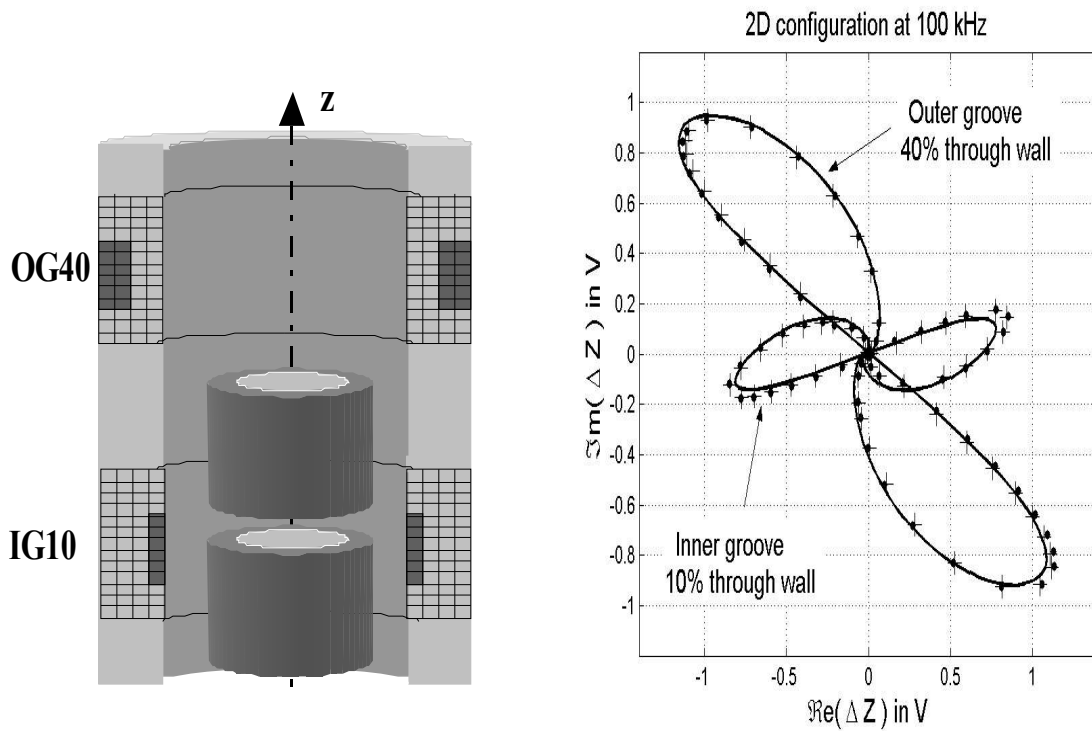
FIGURE 2. Circumferential OG40 and IG10 flaws: schematic and EC signal plane diagram for a centered probe operating at 100 kHz in differential mode ('—' experimental data, '•' 2D model, '+' 3D model).
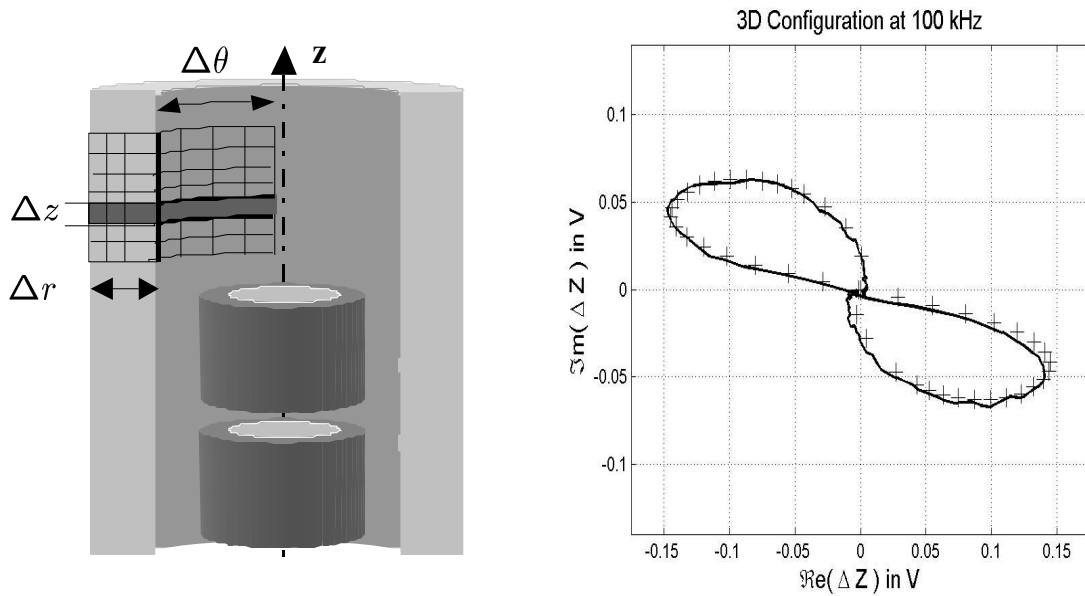
FIGURE 3. Transversal TN100 notch: schematic and EC signal plane diagram for a centered probe operating at 100 kHz in differential mode ('—' experimental data, '+' 3D model).

Figure 3 displays the experimental and simulated EC signal plane diagram obtained with a transversal notch at 100 kHz. This notch (TN100) is a 100% through wall flaw ($\triangle r = 1.27$ mm) of 0.113 mm length ($\triangle z = 0.113$ mm ± 0.020 mm) and of 82° angular extension ($\triangle\theta = 82^o$).

Figure 4 displays the EC signal plane diagram obtained with a longitudinal notch at 100 kHz. This notch (LN54) is a 54% through wall outer flaw ($\triangle r = 0.69$ mm) of 10 mm length ($\triangle z = 10$ mm) and of 0.6° opening ($\triangle\theta = 0.6^o \Leftrightarrow \triangle l = 0.1mm$).
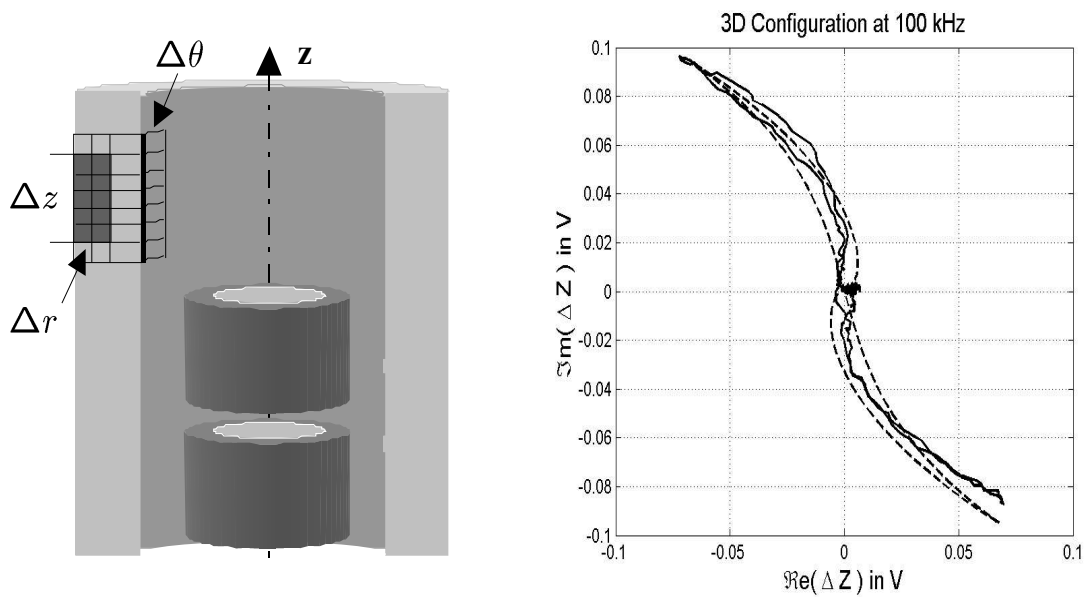
FIGURE 4. Longitudinal LN54 notch: schematic and EC signal plane diagram for a centered probe operating at 100 kHz in differential mode ('—' experimental data, '- -' 3D model).
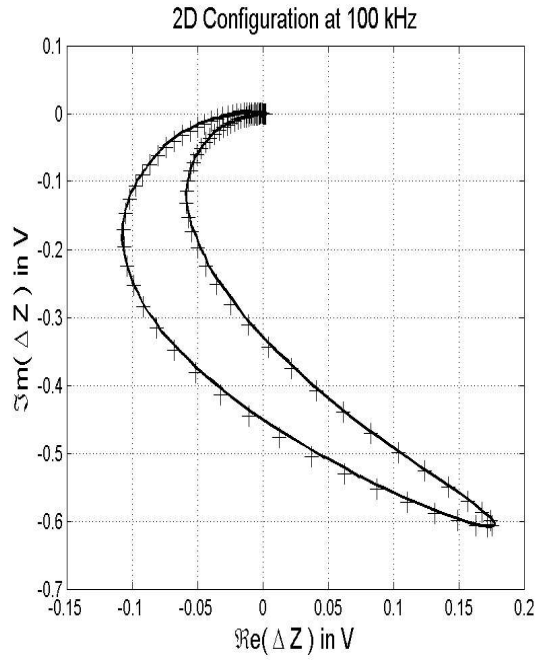
FIGURE 5. Circumferential OG40 flaw: EC signal plane diagram for a centered probe operating at 100 kHz in pseudo absolute mode ('—' experimental data, '+' 3D model).

Figure 5 displays the experimental and simulated EC signal plane diagram obtained at 100 kHz with the OG40 circumferential flaw for a centered probe operating in pseudo absolute mode.

Figure 6 displays the results obtained with the OLG30 circumferential groove and the longitudinal LN54 notch. The OLG30 flaw is a 30% outer through wall groove of 20 mm length ($\triangle z = 20$ mm).
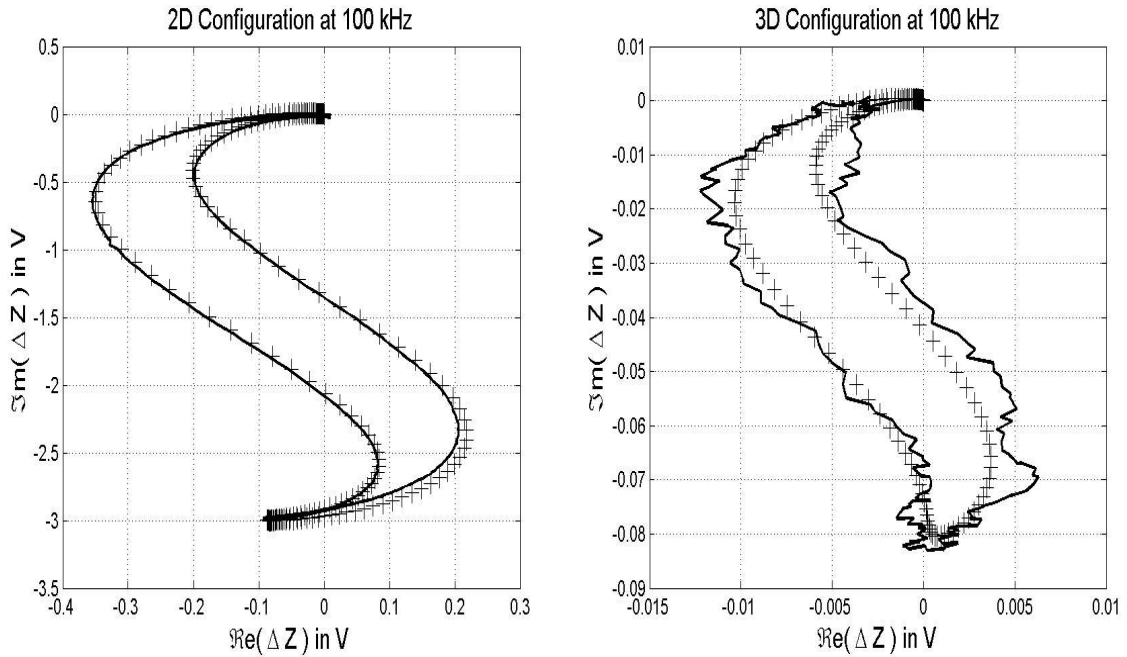
FIGURE 6. Circumferential OLG30 (left) and longitudinal LN54 (right) flaw: EC signal plane diagram for a centered probe operating at 100 kHz in pseudo absolute mode ('—' experimental data, '+' 3D model).
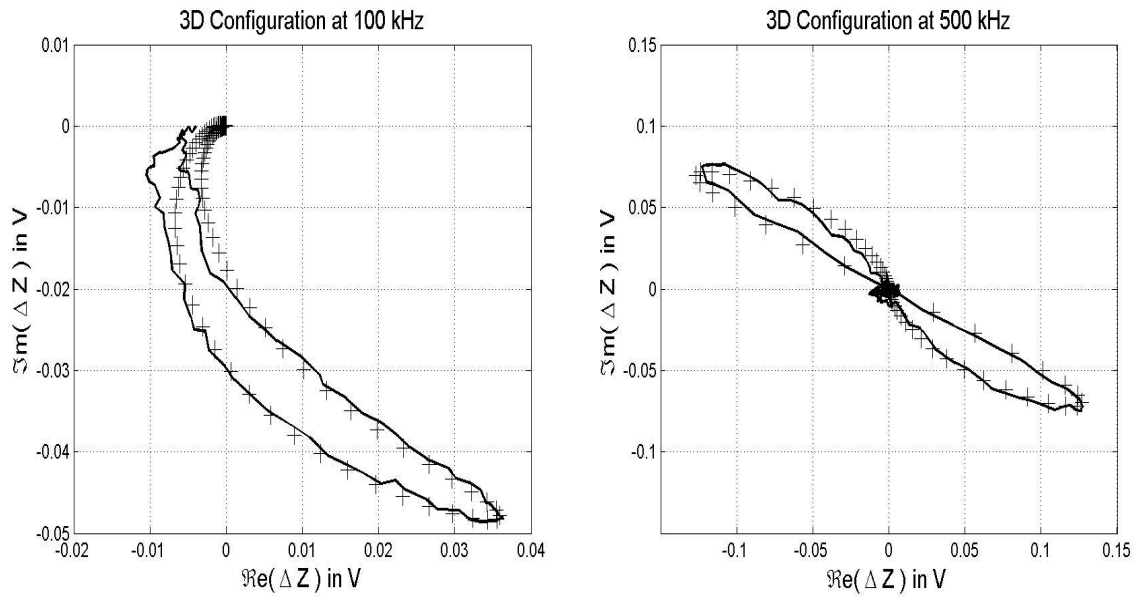
FIGURE 7. Transversal TN100 flaw: EC signal plane diagram for a centered probe operating in pseudo absolute mode (left) at 100 kHz and in differential mode (rigth) at 500 kHz ('—' experimental data, '+' 3D model).

Figure 7 displays the results obtained with the longitudinal TN100 notch. The simulated results were also compared with experimental data at other frequencies. The observed agreements between the results provided by the 3D model and the experimental data are as good as those presented here (for example at 500 kHz, see Figure 7).

Finally, Figure 8 presents typical impedance plane diagram for a non centered probe operating in differential mode for three values of the eccentricity C obtained with a transversal notch. This 3D flaw is a 20% through wall outer notch of 0.1 mm length ($\Delta z = 0.1$ mm) and of 90° opening ($\Delta \theta = 90^o$).
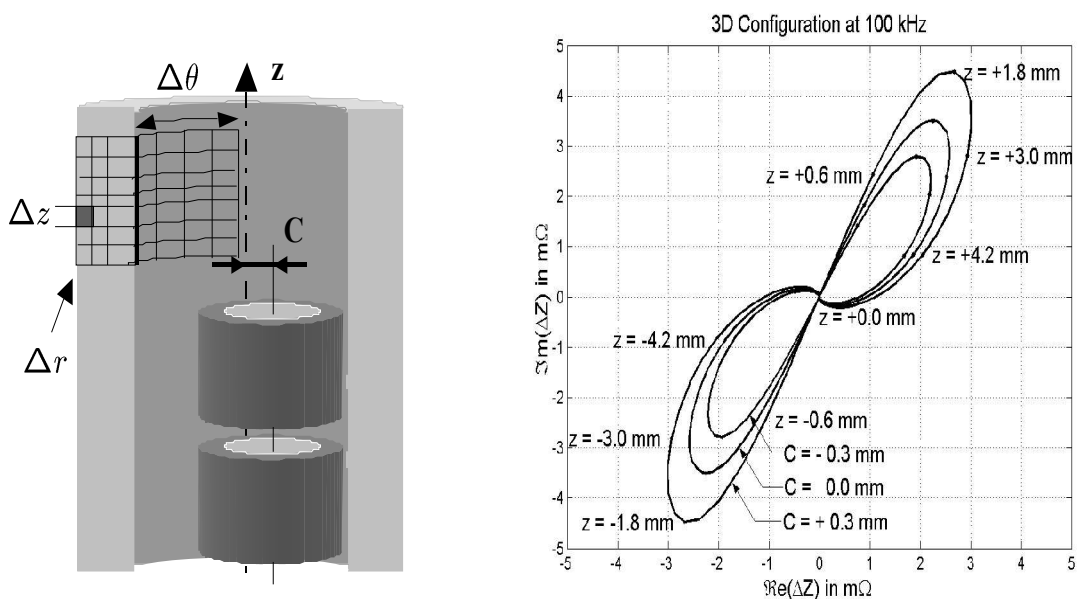
FIGURE 8. Transversal flaw: impedance plane diagram for a non centered probe operating at 100 kHz in differential mode for three values of eccentricity: $C = -0.3$, $C = 0$ mm and $C = +0.3$ mm.

CONCLUSION

A 3D model for eddy current tubing inspection has been developed and a fast numerical code has been implemented. The computing times for the presented EC signal plane diagrams vary from few minutes for 2D configuration up to half an hour for 3D configuration with a 1GHz/1GB PC.

The code may be used to model EC tubing inspection and to study the variations of the probe eccentricity. This 3D model will be integrated in the nondestructive multi techniques platform CIVA.

Good agreements have been observed between experimental and simulated data as well in 2D configurations as in 3D configurations. Further validations will be done considering other flaws (holes …).

The 3D model can be generalized to solve other geometries, in particular, the case of an arbitrary shaped and positioned probe placed outside [8] or inside the tube by changing the incident field computation. Work is presently in progress to simulate, for instance, and eddy current tubing inspection with a pancake coil whose the axis of revolution is perpendicular to the axis of the tube.

REFERENCES

1. Dood, C. V. and Deeds, W. E., *International Journal of Nondestructive Testing* **1**, 29-90 (1968).
2. Sabbagh, H. A. and Sabbagh, L. D., "Development of a System to Invert Eddy-Current Data and Reconstruct Flaws", in *Review of Progress in QNDE Vol. 2*, edited by D. O. Thompson and D. E. Chimenti, Plenum, New York, 1983, pp. 1555-1567.
3. Berthiau, G. and de Barmon, B., "MESSINE, an Eddy Current Parametric Model for Flaw Characterization", in *Review of Progress in QNDE Vol. 18*, edited by D. O. Thompson and D. E. Chimenti, Plenum, New York, 1999, pp. 501-508.
4. Sabbagh, H. A. and Sabbagh, L. D., *IEEE Trans. Magnet.* **MAG-22**, 282-291 (1986)
5. Monebhurrun, V., Duchêne B. and Lesselier D., "Eddy Current Characterization of 3D Bounded Defects in Metal Tubes Using a Wavefield Integral Formulation Modeling", in *Nondestructive Testing of Materials*, edited by R. Collins, W.D. Dover, J.R. Bowler and K. Miya, London, 1995, pp. 195-202.
6. Dyakin, V. V., *Russian Journal of Nondestructive Testing* **33**, 143-153 (1997).
7. Sakaji, N. M., *J. Appl. Phys. D* **33**, 2239-2248 (2000).
8. Micolau, G., Pichenot, G., Lambert, M., Lesselier, D., Premel, D., "Three-Dimensional Electromagnetic Field in a Conductive Cylinder at Eddy-Current Frequencies", in *ENDE'2002 Workshop Proceedings* (to appear).
9. Theodoulidis, T. P., *Res. Nondestr. Eval.* **14**, 111-126 (2002).
10. Chew, W. C., *Waves and Fields in Inhomogeneous Media*, IEEE Press, Piscataway, 1995, Chapters 3, 7 and 8.
11. Li, Y., Zhang, Z., Sun, Y., Udpa, L. and Udpa, S., "Numerical Simulation Results for the Eddy Current Benchmark Problem", in *Review of Progress in QNDE Vol. 21*, edited by D. O. Thompson and D. E. Chimenti, Plenum, New York, 2002, pp. 1902-1908.
12. Tian, Y., Li, Y., Udpa L. and Udpa, S., "Simulation of the World Federation's Second Eddy Current Benchmark Problem", in *Review of Progress in QNDE Vol. 22*, edited by D. O. Thompson and D. E. Chimenti, Plenum, New York, 2002, pp. 1816-1823.